ADVANCED ENGINEERING MATERIALS
www.aem-journal.com

Creep and Superplasticity of Gadolinium-Doped Ceria Ceramics under AC Electric Current

Apurv Dash, Koji Morita, Luca Balice, Robert Mücke, and Olivier Guillon*

Shaping of dense ceramics is difficult due to their inherent brittleness. Nanograined ceramics like tetragonal zirconia (TZP) can be superplastically deformed and shaped at high temperatures owing to grain boundary sliding (GBS). Herein, the enhanced plasticity of gadolinium-doped ceria (GDC) ceramics under mild and strong AC electric current in terms of steady state creep rate under both compressive and tensile loading is demonstrated. A current density of 25 and 200 mA mm^{-2} is used for the creep deformation. The creep rate increases by up to two orders of magnitude under electric current. The stress exponent remains unchanged for creep experiments at 1200 °C with and without electric current, suggesting a GBS mechanism of plastic deformation in both cases. The field-enhanced creep rate is attributed to the interaction of space–charge layer and the electric field resulting in enhanced GBS. A higher current density results in enhanced ductility of GDC even when the Joule heating effect is compensated by reducing the furnace temperature.

1. Introduction

The inherent brittleness of ceramics both at room and high temperature (>1000 °C) has limited its applications and ability to be shaped by hot deformation like metals.[1] Due to small achievable strains, its effect for shaping technology is restricted, for example, the flattening of cambered multilayer compounds.[2] The Maximum achievable strain rates are 10^{-5}–$10^{-4}\,s^{-1}$ for most oxides.[3] In order to enable deformation-based shaping, much larger strain rates yielding considerable strains are required. During research on superplastic ceramics, various oxide ceramics like 3 mol% Y_2O_3-stabilized tetragonal ZrO_2 polycrystals (3Y-TZP),[4,5] Al_2O_3-t ZrO_2-$MgAl_2O_4$ tri-phasic material,[3] $Ca_{10}(PO_4)_6(OH)_2$ hydroxyapatite,[6] fine-grained Al_2O_3,[7] and nonoxide ceramics like Si_3N_4/SiC[8] composites were found to allow much higher strains and strain rates than usual. Strain rates up to 0.01 to $1\,s^{-1}$ with strains of 3–25 were observed.[3,9] The superplastic behavior of ceramics is achieved by grain refinement, a higher grain boundary area ensures grain boundary sliding (GBS), which is one of the major plastic deformation mechanisms of ceramics.[10] However, the temperatures required for carrying out plastic deformation are still very high (typically >1500 °C) with very low permissible rate of deformation to avoid failure except a few high-strain-rate materials.[3] This further limits the economic prospects of superplasticity of submicrometer grained ceramics.[11] Furthermore, the fabrication of submicrometer grained ceramics requires a nanometric primary particle size distribution (<100 nm) as the starting material which further increases the cost and difficulty of the process.

It is known since the 1960s that electrical fields can affect the creep behavior on materials like MgO.[12] For 3Y-TZP, it was found that high field strengths ($E = 1\,kV\,cm^{-1}$) lower the flow stress and thus the viscosity in tensile creep experiments[13] and retard the typical accelerated grain growth and cavitation formation during high-strain-rate creep of ceramics.[14,15] Conrad et al. performed tensile experiments on MgO at $E = 220\,V\,cm^{-1}$ and showed that the flow stress reduced by half with the application of the electrical field.[16] The flow stress recovered reversibly when the field was switched off. Similar behavior was found for 3Y-TZP and Al_2O_3.[13,17] Yoshida et al. applied $120\,V\,cm^{-1}$ on 3Y-TZP samples and achieved a strain of 1.35 using a strain rate of $0.001\,s^{-1}$ at 1000 °C.[18] All these experiments were carried out under tensile loading and under DC fields, which result potentially in single-side reduction of the oxide material when used in field-assisted sintering.

Electric field processing of ceramics peaked interest after Cologna et al. introduced the concept of flash sintering, that is, sintering in a matter of seconds.[19] It was believed that the interaction of electric field with oxide ceramics results in both thermal and athermal effects,[20] the thermal effect being Joule heating and the athermal effects presumably being generation of defects and its concentration along the grain boundary, respectively.[21] The application of electric field resulted in

A. Dash, L. Balice, R. Mücke, O. Guillon
Forschungszentrum Jülich GmbH
Institute of Energy and Climate Research (IEK)
52425 Jülich, Germany
E-mail: a.dash@fz-juelich.de

A. Dash
Department of Energy Conversion and Storage
Technical University of Denmark (DTU)
Building 301, Anker Engelunds Vej, DK-2800 Lyngby, Denmark

K. Morita
Research Center for Functional Materials
National Institute for Materials Science
1-2-1 Sengen, Tsukuba, Ibaraki 305-0047, Japan

The ORCID identification number(s) for the author(s) of this article can be found under https://doi.org/10.1002/adem.202300057.

DOI: 10.1002/adem.202300057

enhanced mass flow and hence the same can be used to induce plastic deformation of ceramics at moderately high temperatures (<1000 °C), which are the typical temperatures of flash sintering for oxide ceramics.[22]

In our previous works we found that all sintering parameters (viscosity, viscous Poisson ratio, sintering stress, bulk, and shear viscosity) of ceria were modified even under moderate AC electrical fields in the order of 10 V cm^{-1}.[23,24] As sintering is governed by grain boundary diffusion which also is a major mechanism for creep in ceramics, it can be expected that these moderate electrical fields also change the creep behavior of ceria. Because of its relevance for membrane, fuel cells, and electrolysis cells, we used submicrometer 10 mol% gadolinia-doped ceria (GDC10) in this work. In the past, it was shown that tensile and compressive loading leads to a symmetric mechanical sintering behavior (sintering and creep are both controlled mainly by grain boundary diffusion in this case).[25] Therefore, the field effect was also studied for tensile and compressive stresses in this work. Many ceramics show asymmetric creep behavior, which is generally attributed to preferential damage under tension, cavitation, or the existence of glassy phases on the grain boundaries.[26–29] The strain development over time was measured at constant stresses with and without electrical field. Considering the window of secondary creep and different stresses, the creep stress exponent was calculated to understand the underlying creep mechanism and the influence of electric current on the same.

The influence of electric field or current on the mechanical properties of oxide ceramics is ultimately due to the power dissipation and hence we have referred to the term "power" or "current" at many instances in the present work. The effect of Joule heating was found to be minor or compensated, suggesting athermal effects of electric current.

2. Results and Discussions

Figure 1a–d shows the typical creep curves of GDC ceramics with (red curve) and without (black curve) electric power under different compressive loading conditions of 20–40 MPa at a furnace

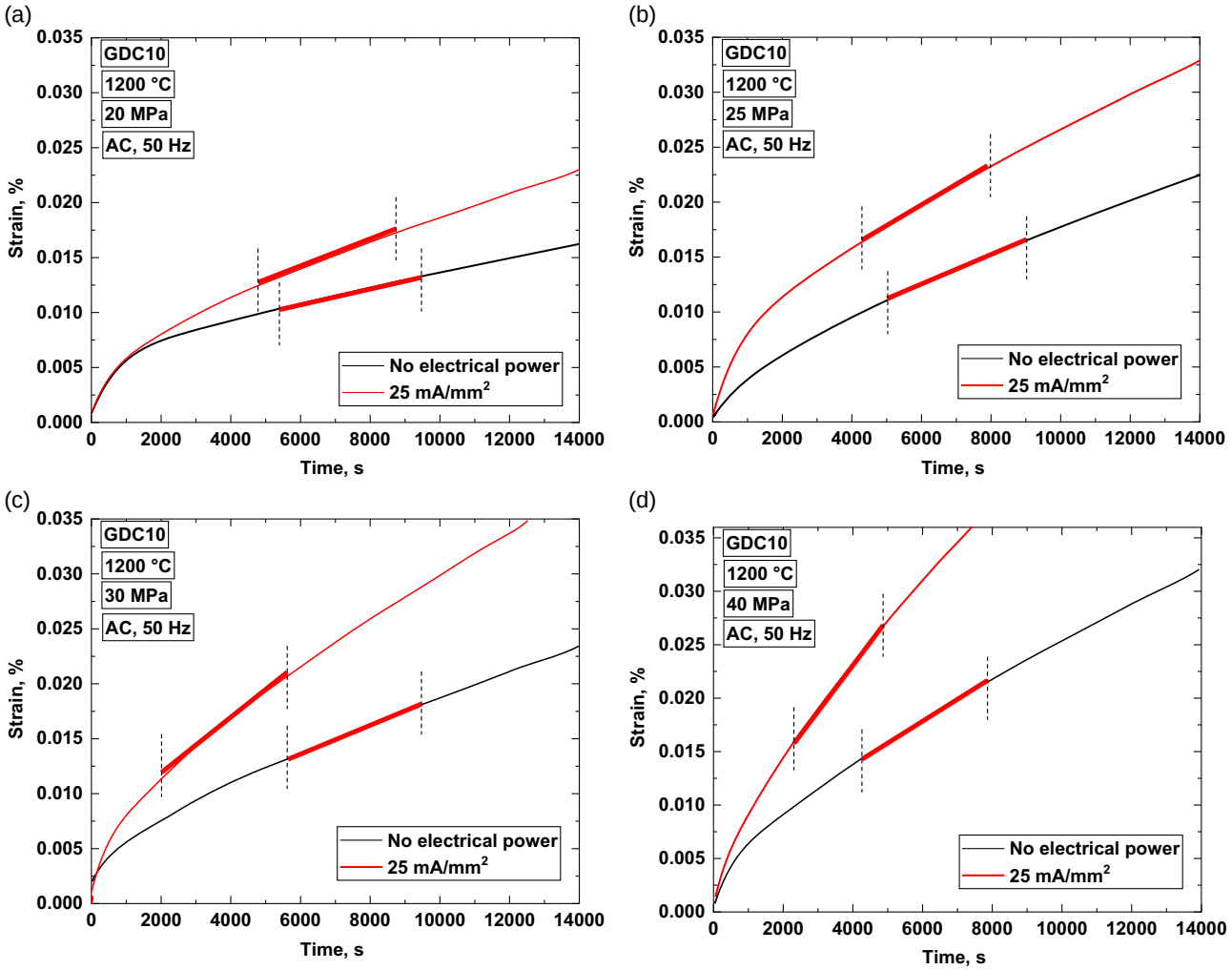

Figure 1. Steady state creep curves under compression of gadolinium-doped ceria under electric field of ≈6 V cm^{-1} and current density of 25 mA mm^{-2} at an isothermal period at 1200 °C a), 10 MPa, b), 20 MPa, c), 30 Mpa, d), 40 MPa.

temperature of 1200 °C. The current density was set to 25 mA mm^{-2} and the electric field self-adjusted to 6.9 V cm^{-1}, resulting in a very low electric power dissipation of 17.25 mW mm^{-3}. The low electric power was used to investigate the effect on creep without triggering Joule heating. A derivative of the creep curve yielded the time window with constant creep rate and the regions are highlighted with a bold red segment in Figure 1. As compressive creep proceeds, the cross section of the cylinder increases as the height reduces and hence hardening takes place. The creep experiments were interrupted once a steady state was reached. The steady state creep rate was measured from the lowest values of the derivative of the strain versus time. A meagre electric power of 17.25 mW mm^{-3} resulted in the increase of creep rate by nearly two times. **Figure 2**a–c shows the creep curves of GDC ceramics under tensile loading. A lower tensile stress was used (10–20 MPa) as ceramics are weak under tensile loading, and this would risk the failure of dog bone samples before testing. The current density was set to 25 mA mm^{-2} and the electric field self-adjusted to 20 V cm^{-1}, resulting in a power dissipation of 50 mW mm^{-3}. The compression tests were performed on cylindrical samples where the platinum electrode was a surface in contact with the flat ends of the cylinder whereas tension tests were performed on a dog bone-shaped sample where the platinum electrode was a point in contact with the hole made at each end of the dog bone. Moreover, the surface area-to-volume ratios for cylindrical and dog bone-shaped samples are very different. We believe that the aforementioned variables like contact resistances and surface area-to-volume ratio are key to the total resistance offered by the sample which in turn reflects the net electric field across the sample. The sample is in a state of redox equilibrium with the ambient oxygen, and increasing surface area-to-volume ratio would drive equilibrium forward and vice versa. The electric field across the ceramic can be assumed to be sample shape dependent. **Table 1** shows a summary of the creep rates in both tensile and compressive modes at 0 and 25 mA mm^{-2}.

Figure 1 and 2 are shown with similar strain window in the *y*-axis and increasing time window on *x*-axis as creep is a time-dependent phenomenon. Strain rate under comparable conditions is always higher for the tensile loading due to sample geometry. The difference is larger than the amount which can be expected from the change in the cross-sectional area during mechanical testing. We observed an intrinsic asymmetric creep behavior common to many ceramics. We can exclude the common reasons for this asymmetry (damage, cavitation, glassy phases).

Table 1. Summary of creep rates in tensile and compressive mode.

Tensile creep		
	Creep strain rate	
Load [MPa]	0 mA mm^{-2}	25 mA mm^{-2}
10	2.31E−05	9.30E−05
15	4.09E−05	1.20E−04
20	9.69E−05	1.26E−04
Compressive creep		
20	5.83E−07	1.10E−06
30	1.30E−06	2.52E−06
40	1.91E−06	4.38E−06
25	1.30E−06	1.95E−06
35	1.94E−06	2.89E−06
50	4.34E−06	7.35E−06

The application of low electric power resulted in negligible Joule heating and an increase in the creep rate at a furnace temperature of 1200 °C. The furnace temperature was lowered to 1100 °C and a higher current density of 200 mA mm^{-2} was applied to induce a Joule heating of around 100 K to have a sample temperature of 1200 °C. A precalibration was done to obtain the corresponding current density for a required increase in temperature of GDC ceramic. **Figure 3** shows the creep curves of GDC ceramics at a furnace temperature of 1100 °C and a sample temperature of 1200 °C. A higher current density resulted in enhanced plasticity of the GDC ceramics. This result is in line with the study of Sasaki et al. for 3Y-TZP.[30] This plastic behavior cannot be attributed to Joule heating as previous experiments done at 1200 °C did not result in the same level of plasticity. All the three stages of creep can be seen in Figure 3 marked with I, II, and III. The first stage is characterized by initial rapid increase in strain, followed by the second stage II, which is the steady-state creep regime where the strain increases linearly with time. In the final stage III, the strain increases rapidly with

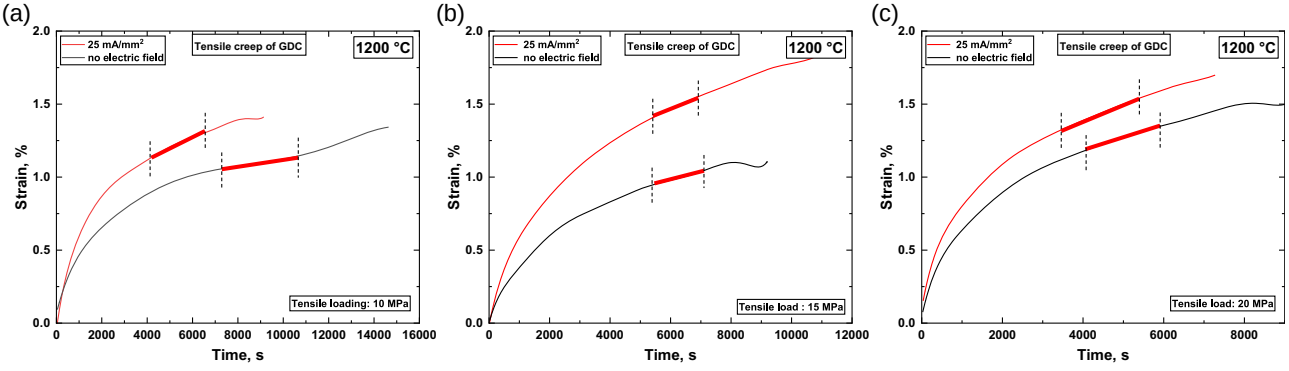

Figure 2. Steady-state creep curves under tension of gadolinium-doped ceria under electric field of ≈20 V cm^{-1} and current density of 25 mA mm^{-2} at an isothermal period at a) 1200 °C, b) 10 MPa, c) 15 MPa, 20 MPa.

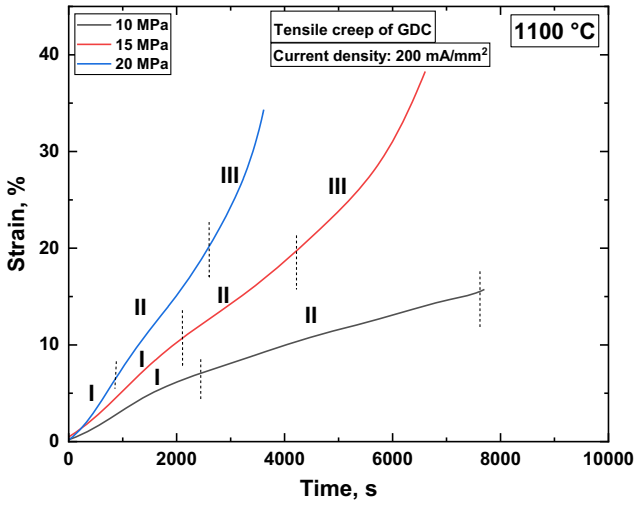

Figure 3. Creep curves of gadolinium-doped ceria under a current density of 200 mA mm^{-2} at an isothermal furnace temperature of 1100 °C under a tensile loading of 10 MPa, 15 MPa, and 20 MPa.

time. The total strain with 200 mA mm^{-2} is much higher (40 %) as compared to that of 25 mA mm^{-2} (<2%).

Figure 4a,b shows the log–log plot of creep strain rate versus the applied stress for compressive and tensile creep experiments, respectively. The application of 25 mA mm^{-2} results in the doubling of the creep rate but slope of the curve depicting the stress exponent remained the same with the applied electric current. The same is true for tensile creep as well, even the injection of a higher current density of 200 mA mm^{-2} resulted in the same stress exponent of ≈2. For the fine-grained materials as in the present material, the deformation behavior characterized by a stress exponent of $n = 2$ has generally been attributed to GBS.[14,31–34] For the deformation of GDC, it would be reasonable to interpret that the flow behavior with $n = 2$ takes place predominantly by GBS, irrespective of the current/field condition, as reported by groups.[33–35] In order to deform continuously by the GBS process, the stress concentrations caused around the multiple grain junctions by GBS should be accommodated by diffusional processes along lattice or grain boundary[31,36] and/or by plastically through dislocation-related processes.[32,37] It has recently been reported that cation diffusivity is likely to be accelerated under the electric current/field.[33–35] This suggests that under electric current/field, the enhanced diffusivity can not only trigger the diffusion-related accommodation process but also the dislocation-related accommodation process by accelerating the recovery rate of dislocations. It is therefore difficult to provide a comprehensive understanding of the predominant rate-controlling mechanisms under the electric current/field. The recent work by D. Liu et al. stated dislocation-related accommodation process as the rate-controlling mechanism under electric current/field based on the transmission electron microscopy (TEM) characterization.[32] If this is the case of the present study, the deformation of GDC can also be ascribed to GBS mechanism, in which the rate of deformation is rate controlled by the dislocation-related processes. Whether the creep mechanism is different below the applied stress of 5 MPa was not studied in the present work as that of Liu et al.[32] The creep rate increases on average by a factor of ≈70 with the applied current density of 200 mA mm^{-2}: The maximum steady-state strain rate was 9×10^{-3} s^{-1} with field compared to 9×10^{-5} s^{-1} without field at 20 MPa. The former is close to the values reported for superplastic ceramics.[11,14,18] This shows the potential of application of the electrical field. If the current density was higher or the grain size was smaller, even full superplasticity can be expected for GDC.[14,30] The stress exponent remained unchanged close to 2, suggesting no modification of the rate-controlling mechanism. The interaction of electric current with the oxide ceramic may have resulted in the change of the grain boundary structure, that is, local reduction along the grain boundary resulting in a high concentration of oxygen vacancies. The accelerated mass flow may also be due to the reduction of grain boundary mobility. The theory of grain growth retardation during electric field-assisted deformation of 3Y-TZP has been well presented by Yang et al.[15] but in the

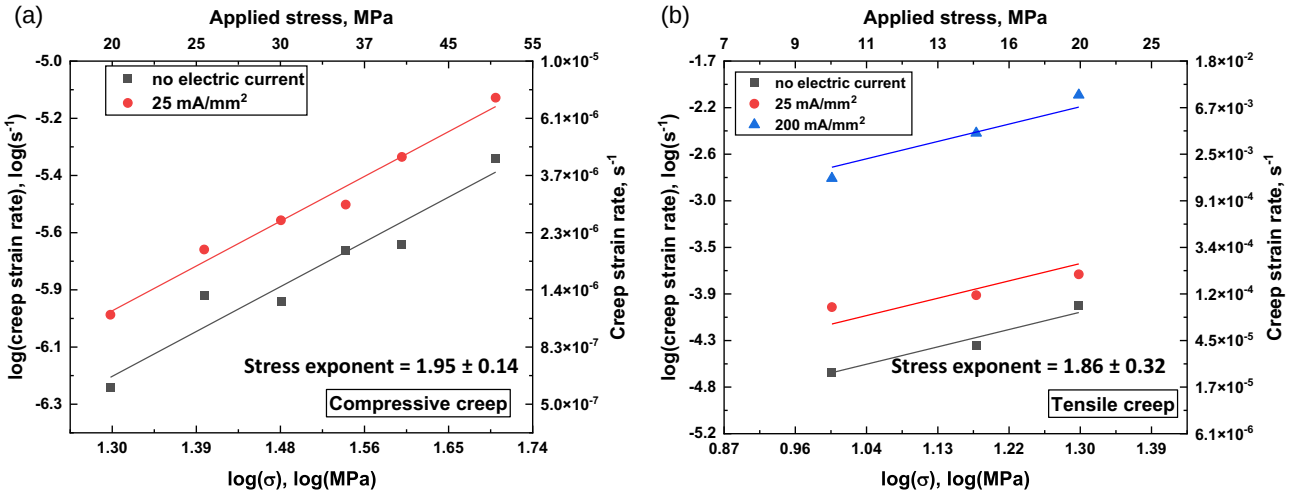

Figure 4. a) Log–log plot of min. creep strain rate as a function of applied compressive stress; b) joule heating of sample as observed with the increase of electric power density in GDC at an isothermal temperature of 1200 °C.

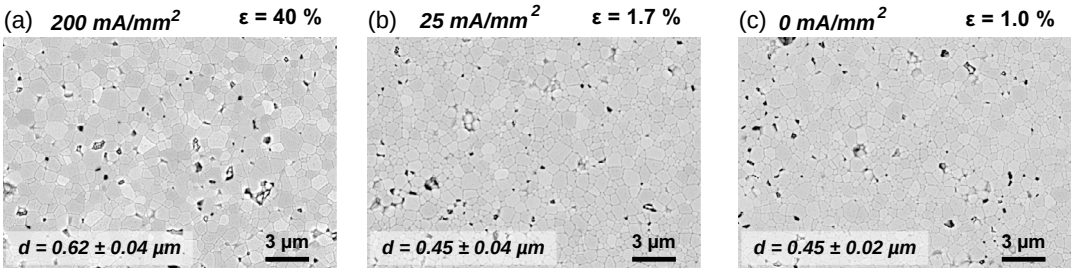

Figure 5. Postcreep microstructure of gadolinium-doped ceria under tensile loading of 15 MPa and current density of a) 200 mA mm^{-2} at 1100 °C, b) 25 mA mm^{-2} at 1200 °C, and c) 1200 °C without any electric field.

present work, the use of electric current did not affect the microstructure, as shown in **Figure 5**. On the contrary, there was a moderate grain growth observed with an increase of current density. The enhanced mass flow might be due to the local grain boundary degradation.[38] However, the use of AC current might have limited the extent of local grain boundary reduction. The reversal of the polarity might lead to a reoxidation of the grain boundary. Previous studies on the electric field-assisted creep and superplasticity were conducted in DC electric field. This might result in a permanently reduced material after deformation, ascribing to the nature of DC current. The present work uses AC electric power, always keeping the system symmetric and lowering the probability of permanent reduction or formation of defects which cannot be annealed by heat treatment in air.

Figure 5 shows the postcreep microstructure of GDC ceramics deformed under 1) 200 mA mm^{-2}, 2) 25 mA mm^{-2}, and 3) without any electric power, deformed under 15 MPa of tensile stress. The microstructure of the sample was investigated both near the electrodes and the core; it was observed that the microstructure is homogeneous. It is noteworthy that a very low degree of cavitation was observed even at a strain level of 40%, suggesting that the GBS is accommodating in nature. With the application of a higher current density, there was a slight grain growth observed (0.62 ± 0.04 µm). This increase in grain size might be due to dynamic grain growth due to grain boundary diffusion accelerated by damage accumulation.[39] The increase in grain size due to the Joule heating can be ruled out as the temperature was only 1200 °C; in addition, if there was an increase in temperature, then it would not have increased beyond 1350 °C which was the sintering temperature of the ceramic. The applied current density cannot result in an increase of temperature over 1350 °C, leading to grain growth. Hence, the grain growth can be ascribed to either current effect or defect accumulation. The grain growth was also symmetric and homogeneous across the gauge length. The application of AC current has been assumed as responsible for enhancing the grain growth without an increase in the sample temperature.[18] The grain size of the ceramic exposed to 25 mA mm^{-2} remained unchanged as compared to the material deformed without electric current and the parent material with a grain size of 0.45 µm. A low current density did not result in a significant defect concentration in the grain boundary to induce grain growth but enough to enhance the GBS phenomenon. This corresponds well to the same sintering trajectories (grain size as function of density) measured during sintering with and without electric field of ceria.[23] The porosity of crept samples under 200 mA mm^{-2} was measured to be 1.2% by image analysis as compared to 0.9% for creep under 25 mA mm^{-2} and 0.7% for creep without electric current. Pore coalescence might have appeared in the case of 200 mA mm^{-2} because of large strain and eventual formation of pores along the grain boundary.[40]

The sample temperature was measured by inserting a thermocouple into a drilled hole in the GDC ceramic for the compression setup. **Figure 6** shows the increase in the sample temperature with increasing power density and current density. It is evident that at a current density of 25 mA mm^{-2} only 5 K of Joule heating was observed. Using a simple black body radiation model

$$P_{\mathrm{el}} = \varepsilon A \sigma (T^4_{\mathrm{sample}} - T^4_{\mathrm{furnace}}) \quad (1)$$

with P_{el} as the dissipated electrical power, ε as emissivity ≈0.9), A the sample area, σ the Stefan–Boltzmann constant, and T the absolute temperate, the sample temperature increase ($T_{\mathrm{sample}} - T_{\mathrm{furnace}}$) was calculated to 21 and 11 K for the compression and tension setup, respectively. These values overestimate the temperature significantly as the mechanical contacts for the mechanical testing conduct substantial heat. A full electrothermal simulation similar to Cao et al.[23] yielded a temperature increase of 1–12 K depending on the position inside the

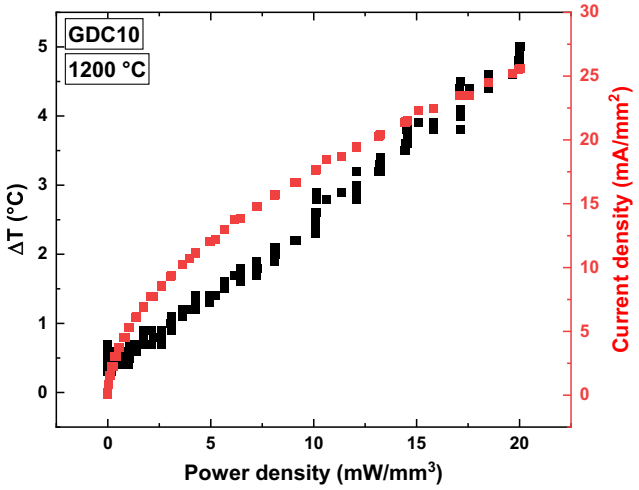

Figure 6. Joule heating of sample as observed with the increase of electric power density in GDC at an isothermal temperature of 1200 °C.

specimen for the compression test. Therefore, an effective increase of the sample temperature of around 5 K for the compression mode is justified and an even small increase took place during the tension test at 25 mA mm^{-2} due to the higher sample surface-to-volume ratio.

The constitutive equation that describes the creep behavior in terms of temperature (T), strain rate ($\dot{\varepsilon}$), applied stress (σ), and grain size (d) is[3,11,18,35,41]

$$\dot{\varepsilon} = A \cdot \sigma^{n} \cdot d^{-p} \exp(-Q/RT) \quad (2)$$

where A, n, p, Q, and R are the material constant, stress exponent, grain size exponent, creep activation energy, and universal gas constant, respectively. An increase in 5 K of the sample would not result in the increase of creep rate by a factor of 2 as seen in the present work. A similar deduction can be made for the creep experiments done with a current density of 200 mA mm^{-2}: a significantly higher creep rate (70 times) cannot be explained by only temperature rise and can be attributed to the interaction of electric power with oxide ceramic and its consequences on the transient change of grain boundary defect chemistry.[38]

3. Conclusion

The creep behavior of gadolinium-doped ceria ceramics was studied under both compressive and tensile loading at 1200 °C with and without the application of electric power. The results show that a higher current density (200 mA mm^{-2}) results in an enhanced mass flow (70 times increased creep rate) as compared to 25 mA mm^{-2} (2 times increased creep rate). The maximum tensile strain rate was found to be 9×10^{-3} s^{-1} for the higher current density. The application of electric power did not result in the change of the rate-controlling factor. Analysis of the postcreep microstructure revealed that a higher current density resulted in moderate cavitation, leading to pore coalescence. The present work showcases that ceria ceramics also exhibit electroplasticity as compared to zirconia- and alumina-based ceramics, which were reported in the past. Especially the use of AC current opens a plethora of new research avenues for the study of electroplasticity of ceria and other ceramics.

4. Experimental Section

Commercial gadolinium-doped cerium oxide ceramics ($Gd_{0.10}Ce_{0.90}O_{1.95}$, Fuel Cell Materials, USA) was used as received. The powders were uniaxially pressed into disks (Ø 30 mm height: 4 mm), cylinders (Ø 20 mm, height: 10 mm) at 50 MPa, followed by isostatic pressing (EPSI, Belgium) at 300 MPa. The pressed pellet was carefully placed in a resistance-heated furnace (Nabertherm, Germany) with a heating ramp of 5 K min^{-1} with a dwell time of 150 min. at 1350 °C to have a relative density above 98% and a grain size below 0.5 µm.

The sintered ceramic was 98.5% dense with a grain size of 0.45 µm. The sintered blocks were machined using diamond tools to obtain cylinders (Ø 4 mm, height: 9 mm) and dog-bone (gauge length: 15 mm, cross-section: 3 mm × 2 mm)-shaped specimen. The cylindrical and dog-bone-shaped specimen were subjected to compressive and tension creep experiments, respectively. Compressive strain was applied by a custom-made sinter forging device[42] equipped with a resistance-heated furnace for heating the sample, a mechanical testing machine (Instron 5565, Norwood, USA) for applying mechanical load, AC power source (ACS-2200, HBS Electronic GmbH, Brühl, Germany) for applying electric bias, and a laser scanner (Model 162-100, Beta Laser Mike, Dayton, USA) to measure the strain of the sample excluding any thermal expansion of the alumina setup for transmitting the load. Platinum plate electrode and wire electrode were used for compression and tension creep, respectively. The sample was painted with platinum paste on both ends to create intimate contact between the ceramic and the electrode. All creep experiments were done under an AC frequency of 50 Hz. The electric current was increased at a rate of 100 mA mm^{-2} min. After the preset current density was reached, the electric field self-adjusted to a certain value to maintain the current density. All the log data from each unit of the setup was recorded using a custom-made LabVIEW program. Tensile strain was applied in a similar setup in which the gauge area of dog-bone samples was clamped in SiC jigs and the displacement was measured by crosshead displacement. The creep investigation was done at 1200 °C in the stress range of 10–50 MPa. Postcreep microstructural investigations (SEM, Zeiss Ultra55, Carl Zeiss, Oberkochen, Germany) were done by grinding and polishing in subsequently finer diamond suspensions and thermal etching at 1100 °C for 30 min.

Acknowledgements

The authors acknowledge funding from the German Science Foundation (DFG), under priority program "Fields Matter" SPP 1959, under the grant no. GU 933/9-2. Dr. Doris Sebold is acknowledged for her help in microscopy of crept samples.

Open Access funding enabled and organized by Projekt DEAL.

Conflict of Interest

The authors declare no conflict of interest.

Data Availability Statement

The data that support the findings of this study are available from the corresponding author upon reasonable request.

Keywords

ceria ceramics, creep, electric current, electro plasticity, grain boundary sliding, plastic deformation

Received: January 12, 2023
Revised: July 14, 2023
Published online: August 8, 2023

[1] W. D. Kingery, H. K. Bowen, D. R. Uhlmann, *Introduction To Ceramics*, John Wiley & Sons, Hoboken **1976**.
[2] R. Mücke, N. H. Menzler, H. P. Buchkremer, D. Stöver, *J. Am. Ceram. Soc.* **2009**, *92*, S95.
[3] B.-N. Kim, K. Hiraga, K. Morita, Y. Sakka, *Nature* **2001**, *413*, 288.
[4] F. Wakai, S. Sakaguchi, Y. Matsuno, *Adv. Ceram. Mater* **1986**, *1*, 259.
[5] K. Kajihara, Y. Yoshizawa, T. Sakuma, *Acta Metall. Mater.* **1995**, *43*, 1235.
[6] F. Wakai, Y. Kodama, S. Sakaguchi, T. Nonami, *J. Am. Ceram. Soc.* **1990**, *73*, 457.
[7] Y. Yoshizawa, T. Sakuma, *Acta Metall. Mater.* **1992**, *40*, 2943.
[8] F. Wakai, Y. Kodama, S. Sakaguchi, N. Murayama, K. Izaki, K. Niihara, *Nature* **1990**, *344*, 421.
[9] K. Hiraga, B.-N. Kim, K. Morita, H. Yoshida, T. S. Suzuki, Y. Sakka, *Sci. Technol. Adv. Mater.* **2007**, *8*, 578.

[10] H. Conrad, *Mater. Sci. Eng. A* **2000**, *287*, 276.
[11] A. H. Chokshi, A. K. Mukherjee, T. G. Langdon, *Mater. Sci. Eng. R: Rep.* **1993**, *10*, 237.
[12] A. S. Neiman, W. S. Rothwell, *Appl. Phys. Lett.* **1963**, *3*, 160.
[13] D. Yang, H. Conrad, *Scr. Mater.* **1997**, *36*, 1431.
[14] K. Hiraga, B.-N. Kim, K. Morita, H. Yoshida, Y. Sakka, M. Tabuchi, *Acta Metall. Sin.* **2011**, *24*, 195.
[15] D. Yang, H. Conrad, *J. Mater. Sci.* **2008**, *43*, 4475.
[16] H. Conrad, D. Yang, *Acta Mater.* **2000**, *48*, 4045.
[17] D. Yang, H. Conrad, *Scr. Mater.* **1999**, *41*, 397.
[18] H. Yoshida, Y. Sasaki, *Scr. Mater.* **2018**, *146*, 173.
[19] M. Cologna, B. Rashkova, R. Raj, *J. Am. Ceram. Soc.* **2010**, *93*, 3556.
[20] H. Masuda, K. Morita, T. Tokunaga, T. Yamamoto, H. Yoshida, *Acta Mater.* **2022**, *227*, 117704.
[21] Y. Dong, I.-W. Chen, *J. Am. Ceram. Soc.* **2018**, *101*, 1058.
[22] M. Biesuz, V. M. Sglavo, *J. Eur. Ceram. Soc.* **2019**, *39*, 115.
[23] C. Cao, R. Mücke, O. Guillon, *Acta Mater.* **2020**, *182*, 77.
[24] C. Cao, R. Mücke, F. Wakai, O. Guillon, *Scr. Mater.* **2020**, *178*, 240.
[25] C. Cao, Y. Sasaki, R. Mücke, K. Morita, O. Guillon, *Scr. Mater.* **2020**, *187*, 137.
[26] E. Blond, N. Schmitt, F. Hild, P. Blumenfeld, J. Poirier, *J. Eur. Ceram. Soc.* **2005**, *25*, 1819.
[27] M. K. Ferber, M. G. Jenkins, V. J. Tennery, in *A Collection of Papers Presented at the 14th Annual Conf. on Composites and Advanced Ceramic Materials: Ceramic Engineering and Science Proceedings*, John Wiley & Sons, Ltd., **1990**, p. 1028.
[28] H. J. Lim, J. W. Jung, D. B. Han, K. T. Kim, *Mater. Sci. Eng. A* **1997**, *224*, 125.
[29] R. S. Kottada, A. H. Chokshi, *Acta Mater.* **2000**, *48*, 3905.
[30] Y. Sasaki, K. Morita, T. Yamamoto, K. Soga, H. Masuda, H. Yoshida, *Scr. Mater.* **2021**, *194*, 113659.
[31] D. M. Owen, A. H. Chokshi, *Acta Mater.* **1998**, *46*, 667.
[32] D. Liu, K. Wang, K. Zhao, J. Liu, L. An, *Scr. Mater.* **2022**, *214*, 114654.
[33] H. Motomura, D. Tamao, K. Nambu, H. Masuda, H. Yoshida, *J. Eur. Ceram. Soc.* **2022**, *42*, 5045.
[34] D. Morikawa, K. Nambu, K. Morita, H. Yoshida, K. Soga, *J. Eur. Ceram. Soc.* **2023**, *43*, 3498.
[35] K. Morita, B.-N. Kim, *J. Eur. Ceram. Soc.* **2022**, *42*, 2341.
[36] I. Charit, A. H. Chokshi, *Acta Mater.* **2001**, *49*, 2239.
[37] K. Morita, K. Hiraga, *Acta Mater.* **2002**, *50*, 1075.
[38] H. Charalambous, S. K. Jha, K. S. N. Vikrant, R. E. García, X. L. Phuah, H. Wang, H. Wang, A. Mukherjee, T. Tsakalakos, *Scr. Mater.* **2021**, *204*, 114130.
[39] B.-N. Kim, K. Hiraga, Y. Sakka, B.-W. Ahn, *Acta Mater.* **1999**, *47*, 3433.
[40] P. E. Evans, *J. Am. Ceram. Soc.* **1970**, *53*, 365.
[41] T. Hiraga, T. Miyazaki, M. Tasaka, H. Yoshida, *Nature* **2010**, *468*, 1091.
[42] E. Aulbach, R. Zuo, J. Rödel, *Exp. Mech.* **2004**, *44*, 71.